Journal of Solid State Chemistry 183 (2010) 1000–1006

Contents lists available at ScienceDirect

Journal of Solid State Chemistry

journal homepage: www.elsevier.com/locate/jssc

Syntheses, structures and properties of 3D inorganic–organic hybrid frameworks constructed from lanthanide polymer and Keggin-type tungstosilicate

Yuanzhe Gao [a,b], Yanqing Xu [a,*], Zhangang Han [a,b], Chunhong Li [a], Fengyun Cui [a], Yingnan Chi [a], Changwen Hu [a,*]

[a] Department of Chemistry, The Institute for Chemical Physics and State Key Laboratory of Explosion Science Technology, Beijing Institute of Technology, Beijing 100081, China
[b] College of Chemistry and Material Science, Hebei Normal University, Shijiazhuang, Hebei 050016, China

ARTICLE INFO

Article history:
Received 17 November 2009
Received in revised form
25 February 2010
Accepted 1 March 2010
Available online 10 March 2010

Keywords:
Polyoxometalates
Lanthanide polymer
Hydrothermal synthesis
Thermal stability
Photoluminescence

ABSTRACT

Inorganic–organic hybrid frameworks, namely $[Ce(H_2O)_3(pdc)]_4[SiW_{12}O_{40}]\cdot 6H_2O$ **1**, $[M(H_2O)_4(pdc)]_4[SiW_{12}O_{40}]\cdot 2H_2O$ (M=Ce for **2a**, La for **2b**, Nd for **2c**; H_2pdc=pyridine-2,6-dicarboxylic acid) were assembled through incorporation of Keggin-type heteropolyanion $[SiW_{12}O_{40}]^{4-}$ within the voids of lanthanides-pdc network as pillars or guests under hydrothermal condition. Single-crystal X-ray analyses of these crystals reveal that compound **1** presents 3D pillar-layered framework with the $[SiW_{12}O_{40}]^{4-}$ anions located on the square voids of the two-dimensional Ce-pdc bilayer. Compounds **2a–c** are isostructural and constructed from 3D Ln-pdc-based metal-organic framework (MOF) incorporating noncoordinating guests Keggin structure $[SiW_{12}O_{40}]^{4-}$. Solid-state properties of compounds **1** and **2a–c** such as thermal stability and photoluminescence have been further investigated.

1. Introduction

Polyoxometalates (POMs), as a unique class of metal-oxide clusters, have provoked significant interest because of their fascinating properties in various fields such as catalysis, biology, magnetism, nonlinear optics, medicine, etc. [1–7]. Over the past two decades, large numbers of POM-based hybrid materials structurally modified by transition metal ions have been heavily investigated [8–19]. However, despite the fundamental and practical significance of the lanthanide complexes, relatively fewer attention has been paid in assisting the self-assembly of POMs building blocks by adopting the rare earth elements as conjunction node [20–23]. It is well known that the oxygen atoms on the surface of POMs are rather active. Highly oxophilic rare earth ions can readily incorporate with POMs and O-donor organic ligands. Thus, when choosing appropriate bridging ligands capable of connecting rare earth centers with POMs building block, it is possible to construct Ln-POMs framework via direct bond formation or hydrogen-bonding interactions. Pyridine-2,6-dicarboxylic (H_2pdc), possessing relatively high coordination sites, small volume and versatile coordination behaviors, is proved to make appreciable polymeric metal-organic moieties fitting for the combination of POM subunits with 4*f* metals, and aroused our attention [20]. In our newly reported work, we have succeeded in assembling a series of novel Ln-pdc frameworks with Zeolite Gismondine topology holding polyoxometalate counterions $[XMo_{12}O_{40}]^{4-}$ (X=Si and Ge) in their cavities [22]. In our sequential work here, we turned to $[SiW_{12}O_{40}]^{4-}$ for its better stability, and obtained four new lanthanide-linked compounds based on $[SiW_{12}O_{40}]^{4-}$ entity. Among them, compound **1** displays the pillar-layered architectures with the polyoxometalate functioned as the pillar, and compounds **2a–c** are isostructural and show 3D Ln-pdc-based metal-organic framework (MOF) involving noncoordinating guests Keggin structure $[SiW_{12}O_{40}]^{4-}$ within their channel. Further more, the IR, UV–vis, powder X-ray diffraction (PXRD), thermogravimetric analysis (TGA) and photoluminescent properties of the compounds have been investigated in this work. These compounds represent the successful examples of 4*f* metal ions instead of transition ones assembled with $[SiW_{12}O_{40}]^{4-}$ species.

2. Experimental

2.1. Materials and methods

All the chemical materials purchased for synthesis were of reagent grade and used without further purification. Elemental

* Corresponding authors. Fax: +86 10 68912631.
E-mail addresses: xyq@bit.edu.cn (Y. Xu), cwhu@bit.edu.cn (C. Hu).

0022-4596/$ - see front matter © 2010 Elsevier Inc. All rights reserved.
doi:10.1016/j.jssc.2010.03.006

analyses were performed on a Perkin-Elmer 2400 element analyzer and inductively coupled plasma analysis on a Perkin-Elmer Optima 3300DV ICP spectrometer. IR (infrared) spectra were recorded in the range of 4000–400 cm^{-1} on a Nicolet 170SXFT/IR spectrometer (as KBr pressed pellets). PXRD (powder X-ray diffraction) of samples were collected on a Japan Rigaku *D*/max γA X-ray diffractometer equipped with graphite monochromatized Cu*K*α radiation (λ=0.154060 nm). Emission/excitation spectra were obtained on a Hitachi F-4500 fluorescence/phosphorescence spectrophotometer, and the measurements were performed at room temperature. TGA (thermogravimetric analysis) curves were carried out on a 2960 SDT simultaneous thermal analyzer under nitrogen atmosphere from room temperature to 800 °C with a heating rate of 10 °C/min. Hydrothermal syntheses were carried out in 18 mL Teflon-lined autoclaves under autogenous pressure.

2.2. Synthesis

2.2.1. Synthesis of $[Ce(H_2O)_3(pdc)]_4[SiW_{12}O_{40}]\cdot 6H_2O$ (**1**)

A mixture of $H_4SiW_{12}O_{40}$ (0.25 mmol, 0.72 g), H_2pdc (0.25 mmol, 0.042 g), $Ce(NO_3)_3\cdot 6H_2O$ (0.25 mmol, 0.108 g), NH_4VO_3 (0.5 mmol, 0.059 g) and H_2O (8 mL) were stirred for about 1 h in air. Then the pH value was adjusted to 2–3 by dense NaOH. The mixture was transferred and sealed in an 18 mL Teflon-lined autoclave and kept at 160 °C for 72 h, yellow sheet-like crystals of **1** were collected after filtration, washed with distilled water, and dried at ambient temperature. Yield: ~20% (based on W). Elemental analysis (%). Anal. calcd. for $C_{28}H_{48}Ce_4N_4O_{74}SiW_{12}$ (4419.44): C, 7.61; H, 1.09; N, 1.27; Si, 0.64; Ce, 12.68; W, 49.92%. Found: C, 7.58; H, 1.20; N, 1.31; Si, 0.71; Ce, 12.71; W 50.02 (%). IR (KBr, cm^{-1}) *v*: 3463 (s), 1609 (vs), 1563 (vs), 1447 (s), 1398 (s), 1377 (m), 1280 (m), 1199 (w), 1077 (m), 1016 (w), 969 (s), 916 (vs), 883 (w), 802 (vs), 762 (vs), 697 (w), 661 (w), 537 (w).

2.2.2. Synthesis of $[Ce(H_2O)_4(pdc)]_4[SiW_{12}O_{40}]\cdot 2H_2O$ (**2a**)

Compound **2a** was prepared in the same way as **1**, except the pH value was increased to 4.5 by adding dense NaOH solution. Orange block crystals were obtained. Yield: ~54% (based on W). Anal. calcd. for $C_{28}H_{48}Ce_4N_4O_{74}SiW_{12}$ (4419.44): C, 7.61; H, 1.09; N, 1.27; Si, 0.64; Ce, 12.68; W, 49.92 (%). Found: C, 7.58; H, 1.08; N, 1.21; Si, 0.70; Ce, 12.75; W 49.82 (%). IR (KBr, cm^{-1}) *v*: 3471 (s), 1608 (vs), 1566 (vs), 1448 (s), 1398 (s), 1382 (m), 1282 (m), 1194 (w), 1072 (m), 1018 (w), 970 (s), 918 (s), 885 (m), 802 (vs), 763 (vs), 698 (w), 662 (w), 536 (w).

2.2.3. Synthesis of $[La(H_2O)_4(pdc)]_4[SiW_{12}O_{40}]\cdot 2H_2O$ (**2b**)

Compound **2b** was prepared in the same way as **2a**, except using $La(NO_3)_3\cdot 6H_2O$ to replace $Ce(NO_3)_3\cdot 6H_2O$. Orange block crystals were obtained. Yield: ~75% (based on W). Anal. calcd. for $C_{28}H_{48}La_4N_4O_{74}SiW_{12}$ (4414.58): C, 7.62; H, 1.10; N, 1.27; Si, 0.64; La, 12.59; W, 49.98 (%). Found: C,7.60; H, 1.14; N, 1.27; Si, 0.70; La, 12.65; W, 50.28 (%). IR (KBr, cm^{-1}) *v*: 3469 (s), 1609 (vs), 1564 (vs), 1447 (s), 1396 (s), 1381 (m), 1280 (m), 1197 (w), 1069 (m), 1017 (w), 970 (s), 914 (s), 882 (m), 802 (vs), 761(vs), 695 (w), 665 (w), 535 (w).

2.2.4. Synthesis of $[Nd(H_2O)_4(pdc)]_4[SiW_{12}O_{40}]\cdot 2H_2O$ (**2c**)

Compound **2c** was prepared in the same way as **2a**, except using $Nd(NO_3)_3\cdot 6H_2O$ to replace $Ce(NO_3)_3\cdot 6H_2O$. Orange block crystals of **2b** were collected by filtration, washed with distilled water, and dried at ambient temperature. Yield: ~62% (based on W). Anal. calcd. for $C_{28}H_{48}Nd_4N_4O_{74}SiW_{12}$ (4435.92): C, 7.58; H, 1.09; N, 1.26; Si, 0.63; Nd, 13.01; W, 49.73. Found: C, 7.55; H, 1.14; N, 1.21, Si, 0.71; Nd, 12.91; W, 50.01 (%). IR (KBr, cm^{-1}) *v*: 3474 (s), 1609 (vs), 1565 (vs), 1450 (s), 1398 (s), 1377 (w), 1281 (m), 1194 (w), 1074 (m), 1016 (w), 970 (vs), 916 (s), 884 (m), 803 (vs), 763 (vs), 697 (w), 662 (w), 537 (w).

2.3. X-ray crystallography

Single-crystal X-ray diffraction data for compounds **1** and **2a–c** were collected at 298 K on a Bruker-AXS CCD diffractometer equipped with a graphite-monochromated Mo*K*α radiation (λ=0.71073 Å). All absorption corrections were applied using multi-scan technique. All the structures were solved by the direct method of SHELXS-97 [24] and refined by full-matrix least-squares techniques method on F^2 using the SHELXTL crystallographic software package [25]. Anisotropic thermal parameters were used to refine all non-hydrogen atoms in **1–2b**. But in **2c**, Si atom is just refined in isotropic way for poor data quality. The hydrogen atoms of the organic ligands were refined as rigid groups. All water H atoms in compounds **1** and O1w in **2b** could not be positioned reliably. The disordered polyoxoanions in compound **1** were refined using O (center oxygen) atoms split over two equivalent sites. The detailed crystallographic data and structure refinement parameters for **1**, **2a–c** are summarized in Table 1. Selected bond angles and lengths of **1**, **2a–c** are listed in Supplementary (see Table S1). Crystallographic data for the structures reported in this paper have been deposited in the Cambridge Crystallographic Data Center with CCDC reference numbers 753,523–753,526 for compounds **1 and 2a–c**, respectively.

3. Results and discussion

3.1. Synthesis consideration

The synthesis route is generalized in Scheme 1. The hydrothermal temperature and metal–ligand molar ratio in aqueous solution do not have obvious influence on the final product, though the yields did vary somewhat. But the pH of the reaction system has a decisive impact on the formation of the final product. When $Ce(NO_3)_3\cdot 6H_2O$ and other same raw starting materials are selected, compounds **1** and **2a** were isolated at different pH of 2–3 and 4.5, respectively. When the metal salts are altered from $Ce(NO_3)_3\cdot 6H_2O$ to $La(NO_3)_3\cdot 6H_2O$ and $Nd(NO_3)_3\cdot 6H_2O$ at pH of 4.5, **2b** and **2c** were obtained. However, though many parallel experiments were done at pH of 2–3, species containing La and Nd have not been isolated so far. In addition, it is worth noting that NH_4VO_3 is a necessary ingredient for the successful isolation of these four compounds in spite of its absence from the resultant crystal structures. We surmised that the NH_4VO_3 affects the formation of the cluster for the characteristic comparability of identical group elements though its role is not clear yet [26,27].

3.2. Description of crystal structures

Single crystal X-ray diffraction analysis reveals that compound **1** contains two crystallographically independent Ce(III) cations, one Keggin-type $[SiW_{12}O_{40}]^{4-}$ (SiW_{12}) anion, two H_2pdc ligands, six coordinated water molecules and other three free lattice water molecules. The SiW_{12} anion exhibits a classical α-Keggin configuration (Fig. S1). The central atom Si is disorderly surrounded by a cube of eight oxygen atoms, with each oxygen site half-occupied, as has been observed in previous literatures [28]. The Si–O distances range from 1.50(9) to 1.74(9) Å. Each W atom shows a {WO_6} octahedral environment and the W–O bond

Table 1
Crystal data and structure refinement for **1–2c**.

Compounds	1	2a	2b	2c
Formula	C_{28} H_{48} Ce_4 N_4 O_{74} Si W_{12}	C_{28} H_{48} Ce_4 N_4 O_{74} Si W_{12}	C_{28} $H_{48}La_4$ N_4 O_{74} SiW_{12}	C_{28} H_{48} N_4 Nd_4 $O_{74}Si$ W_{12}
Formula weight	4419.44	4419.44	4414.58	4435.92
Crystal system	Triclinic	Tetragonal	Tetragonal	Tetragonal
Space group	$P-1$	$I4(1)/a$	$I4(1)/a$	$I4(1)/a$
a (Å)	11.7554(13)	21.999(2)	21.8937(19)	21.917(2)
b (Å)	14.4359(16)	21.999(2)	21.8937(19)	21.917(2)
c (Å)	14.6933(17)	16.7023(15)	16.7687(15)	16.5868(18)
α (deg)	111.146(2)	90	90	90
β (deg)	112.698(2)	90	90	90
γ (deg)	93.2150(10)	90	90	90
V (Å^3)	2089.5(4)	8083.3(14)	8037.8(12)	7967.2(15)
Z	1	4	4	4
Dc (g cm)	3.509	3.632	3.645	3.758
μ(Mo$K\alpha$) (mm^{-1})	18.701	19. 336	19.306	19.946
Reflections collected	10,083	16,614	18,968	15,710
Independent reflns	7048 [R(int)=0.0795]	3543 [R(int)=0.1048]	3537 [R(int)=0.0966]	3512 [R(int)=0.1235]
Data/parameters	7048/574	3543/278	3537/269	3512/278
GoF on F^2	1.014	1.150	1.141	1.125
R^a[$I > 2\sigma(I)$]	$R1$=0.1202, wR_2=0.2915	$R1$=0.0578, w$R2$=0.1398	$R1$=0.0359, w$R2$=0.0837	$R1$=0.0610, w$R2$=0.1257
R^b [all data]	$R1$=0.2017, wR_2=0.3379	$R1$=0.0731, w$R2$=0.1509	$R1$=0.0552, w$R2$=0.0997	$R1$=0.0971, w$R2$=0.1472

[a] $R_1=\Sigma\ |\ |F_o|-|F_c|\ |/\Sigma\ |F_o|$.
[b] $wR_2=\{\Sigma\ [w\ (F_o^2-F_c^2)^2\ ]/\Sigma\ [w\ (F_o^2)^2]\}^{1/2}$.

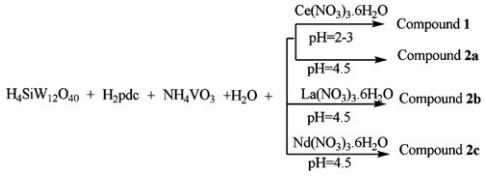

Scheme 1. Synthesis of compounds **1–2c.**

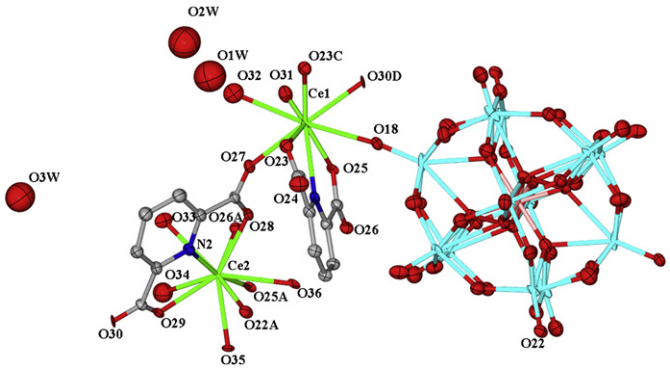

Fig. 1. ORTEP view of the asymmetric unit in compound **1**. The Keggin anions are drawn completely for clarity. The thermal ellipsoids are drawn at 50% probability. Only parts of atoms are labeled, and all the hydrogen atoms are omitted for clarity. Symmetry code: A: $1-x$, $1-y$, $-z$; B: $x-1$, y, z; C: 2-x, $1-y$, $1-z$; D: $1+x$, y, z.

distances fall in the ranges 1.60(4)–1.77(4) Å, 1.80(3)–2.01(4) Å and 2.25(6)–2.49(6) Å, and the mean values are 1.67(4), 1.91(4) and 2.40(6) Å, respectively, which are within the normal ranges and in close agreement with those described in the literature [29]. As shown in Fig. 1, Ce1 ion is nine-coordinated by three water molecules, four carboxyl oxygen atoms from three different dpc^{2-} ligands [Ce1$-O_{pdc}$=2.53(3)–2.63(3) Å], one oxygen atom of the Keggin $[SiW_{12}O_{40}]^{4-}$ polyoxoanion and one nitrogen atom from the H_2dpc ligand, respectively. Ce2 ion displays the ten-coordination geometry coordinated by four water molecules, four oxygen atoms from two H_2dpc ligand and one nitrogen atom from H_2dpc ligand and one oxygen atom of the Keggin $[SiW_{12}O_{40}]^{4-}$ polyoxoanion. As shown in Fig. 2, X-ray crystallography reveals that Ce1 and Ce2 are ligated by the incorporation of O25–O30 from different carboxyl groups of pdc and generate 1D zigzag double-chain structure along a direction (O25–Ce1 2.53(3); O27–Ce1 2.56(3); Ce2–O28 2.55(3); Ce2–O29 2.61(3); Ce2A–O25 2.99(3); Ce1B–O30 2.53(3) Å). Then the neighboring double-chains are further linked together by two symmetry-related O23 and O23C from pdc ligands to form a flexural 2D Ln-pdc sheet along the ac plane (Ce1–O23 2.63(3), Ce1–O23C 2.66(3)). Furthermore, the two adjacent layers are connected by the covalent bonding of terminal O18 and O22 of the Keggin clusters to the double chain with the O18–Ce1 distance being 2.80(3), Ce2–O22 2.66(3) Å to give rise to a 3D neutral network. In other words, these positive charged 2D Ce-pdc sheets are pillared by the $[SiW_{12}O_{40}]^{4-}$ anions to form 3D microporous pillar-layered framework containing "guest" water molecules (see Fig. 3). As a result of covalent bonding interactions between the polyoxoanions and metal-organic cations, the pillar $[SiW_{12}O_{40}]^{4-}$ entity props up the framework with void of ca. 5.6×4.4 Å. Analysis with the PLATON19 software tool indicates that the volume per unit cell is approximately 8.6% (in the absence of free water molecules) [30,31].

Compounds **2a–c** are isostructural and represent 3D non-interwoven frameworks. Here, only **2a** is described in detail. Different from the case in **1**, the Keggin $[SiW_{12}O_{40}]^{4-}$ entities function as guest to occupy the distorted-honeycomb cavities in compound **2a**. The well-known SiW_{12} anion exhibits a classical α-Keggin configuration. The central atom Si is surrounded by four oxygen atoms, with each oxygen site whole-occupied (see Fig. S2). Each Ce^{3+} cation is coordinated in a distorted-square-antiprismatic geometry by four water ligands, four oxygen atoms from three independent pdc ligands and one nitrogen atom from a pdc ligand. As shown in Fig. 4a, four nine-coordinated Ce^{3+} ions are linked by carboxylate groups of four pdc ligands to form a tetranuclear cyclic unit $\{[Ce(H_2O)_4(pdc)]_4\}^{4+}$. Two tetranuclear cyclic units chelate one $[SiW_{12}O_{40}]^{4-}$ ion through O–H$\cdots$O hydrogen bonding (Fig. 4c, Table 2). In addition, an octanuclear metallamacrocycle composed of $Ce_8(pdc)_8$ also can be abstracted from the topology (see Fig. 4b). Thus, a 3D lanthanide-organic

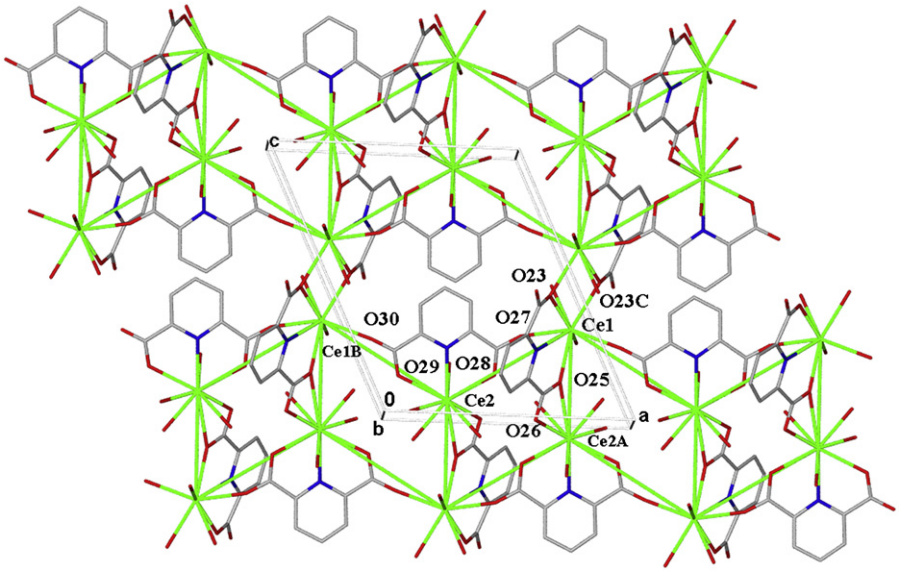

Fig. 2. View of the flexural 2D Ln-pdc sheet network in **1** along the *ac* plane formed by linking of the neighboring zigzag double-chains; all H atoms are omitted for clarity.

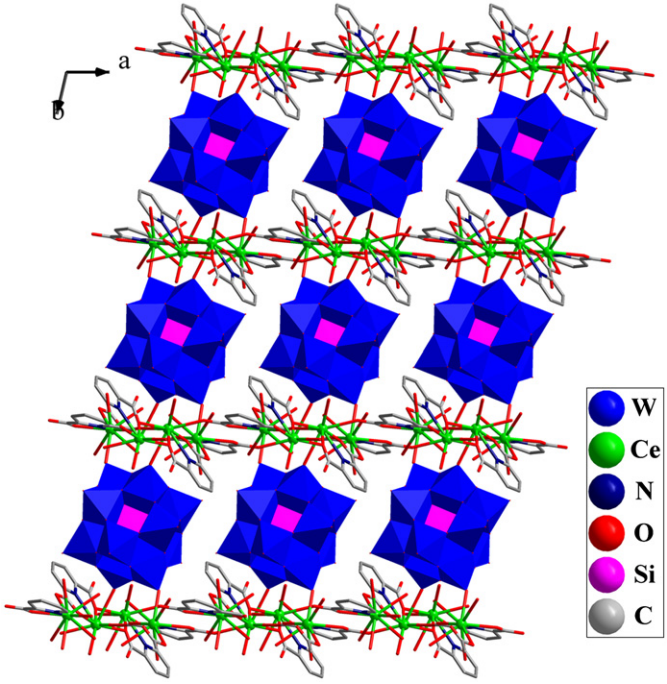

Fig. 3. Packing of the 3D pillar-layered framework in compound **1**. All the water molecules trapped into the channels are omitted for clarity.

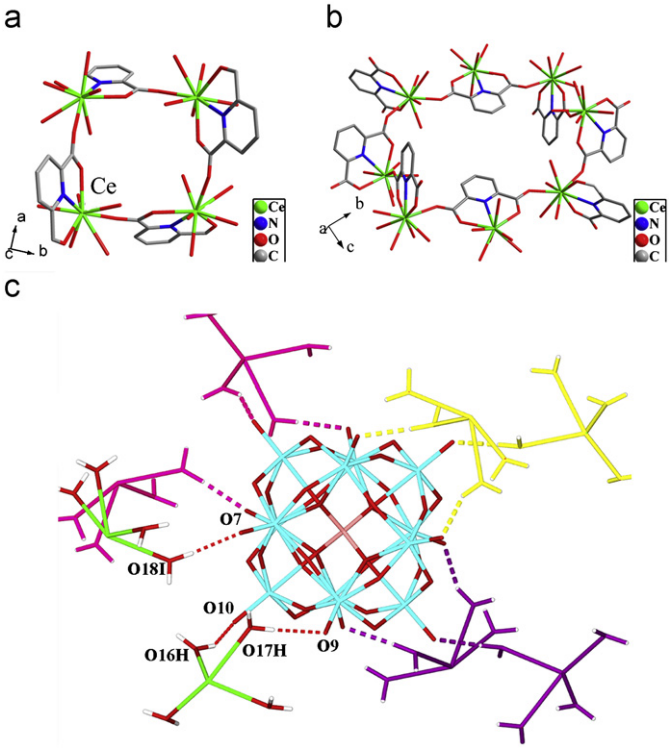

Fig. 4. (a) Structure of the tetranuclear cyclic unit and (b) octanuclear cyclic unit in compound **2a**. (c) View of the hydrogen bonds between two tetranuclear cyclic units $\{[Ce(H_2O)_4(pdc)]_4\}^{4+}$ and $[SiW_{12}O_{40}]^{4-}$ ions in **2a**. The pdc ligands are omitted for clarity. Four kinds of color represent four sets of H-bonding intersections. Symmetry code: H $5/4-y, x-1/4, 3/4+z$; I $x, y, 1+z$.

cationic architecture is built up from the tetranuclear cyclic units and octanuclear metallamacrocycles (Fig. S3). Further, eight-member channels would be found along the *c*-axis directions in the 3D cationic network of **2a** (see Fig. S3b). The four-membered rings, $\{[Ce(H_2O)_4(pdc)]_4\}^{4+}$, can be also treated as the unit of the double-crankshaft chain (cc). Thus a Ce^{3+} center can be viewed as four-connected node to form a 3D uninodal cationic network with Schläfli symbol of $(4^3 \cdot 6^2 \cdot 8)$, which is related to the structural prototype of natural zeolite GIS [32,33] (see Fig. S4). These channels intersect each other to form large cavities, which array in a zigzag fashion and are occupied by nanosized $[SiW_{12}O_{40}]^{4-}$ counterions (Fig. 5).

3.3. Characterization of compounds

3.3.1. Infrared spectra

Based on bond valence sum calculations and charge balance consideration, all W and Ln centers exhibit the +6 and +3 oxidation states, respectively [34]. As shown in Fig. S5, the IR spectra of **1** and **2a** demonstrate the characteristic bands of the

Table 2
Hydrogen bond lengths (Å) and angles (deg) in **2a**.[a]

D–H···A	d(D–H) (Å)	d(H···A) (Å)	d(D···A) (Å)	<(DHA) (deg)
O(16)–H(16C)···O(10E)	0.85	1.98	2.75(2)	149.6
O(17)–H(17C)···O(9E)	0.85	1.99	2.84(2)	176.8
O(18)–H(18C)···O(7F)	0.85	1.96	2.81(2)	176.0
O(15)–H(15C)···O(14)	0.85	1.93	2.73(2)	156.2
O(18)–H(18D)···O(12G)	0.85	1.82	2.66(2)	175.9

[a] Symmetry codes for **2a**: E: $y+1/4,-x+5/4,z-3/4$; F: $x,y,z-1$; G: $x-1/2,y,-z+1/2$.

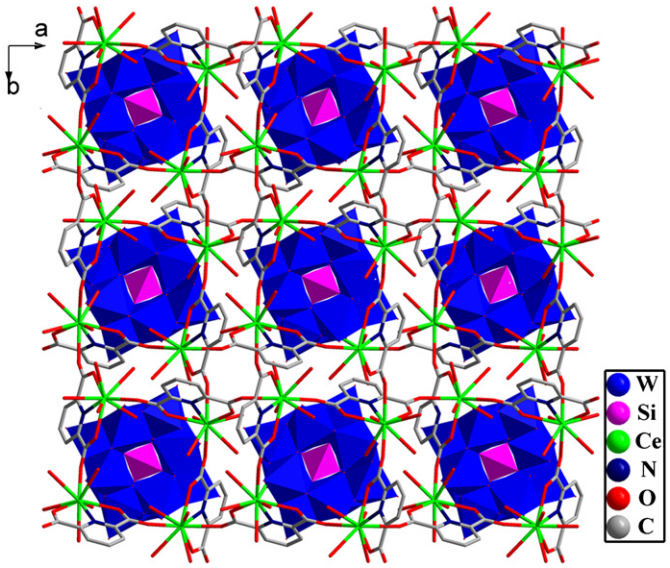

Fig. 5. The cavities of intersected channels occupied by $[SiW_{12}O_{40}]^{4-}$ counterions. All the hydrogen atoms and the water molecules trapped into the channels are omitted for clarity. Blue polyhedra: $[SiW_{12}O_{40}]^{4-}$.

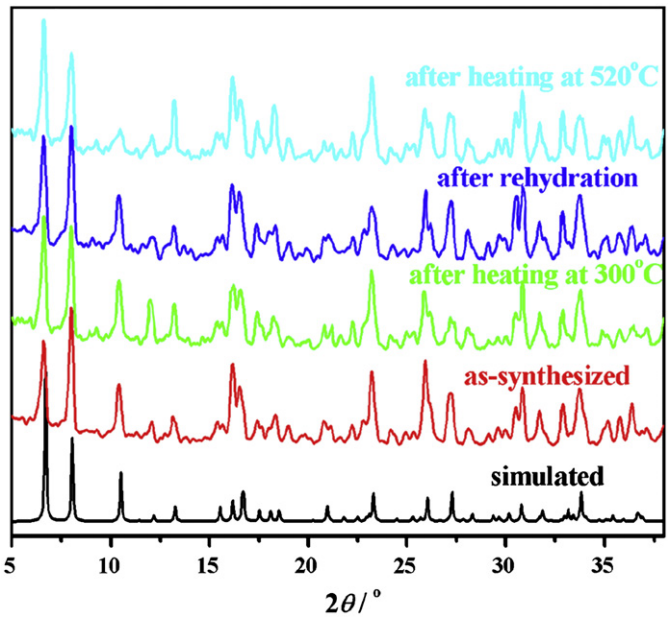

Fig. 6. The powder X-ray diffraction patterns after heating of compound **2a**.

Keggin tungstosilicate with little differences between these two compounds. Four characteristic peaks at 1077, 969, 916, 762 cm^{-1} in **1**, and 1072, 970, 918, 763 cm^{-1} in **2a**, are attributed to the ν_{as}(Si–O_a), ν_{as}(W–O_d), ν_{as}(W–O_b–W) and ν_{as}(W–O_c–W) stretching vibration, respectively. Compared with the typical Keggin-type parent $H_4SiW_{12}O_{40}$ [35], these results demonstrate that the SiW_{12} clusters are slightly shifted, the reason of which may be that the interactions between the clusters and $[Ln(H_2O)_{3-4}(pdc)]_4^{4+}$ subunits, which indicates that the new complexes still retain the basic frame of the Keggin structure. The broad bands of 3463 cm^{-1} for compound **1** and 3471 cm^{-1} for compound **2a** characterize water molecules. The characteristic peaks at 1609, 1563, 1447, 1398, 1377, 1280 cm^{-1} in **1** and 1608, 1566, 1448, 1398, 1382, 1282 cm^{-1} in **2a** can be regarded as features of the H_2pdc molecules. However, in comparison with the IR spectra of the H_2dpc, the vibration frequencies of ν(C=O), ν(C=N), ν(C–O) in **1** and **2a** have red-shifted, the reason of which may be the effect of coordination between N atom and Ln center.

3.3.2. UV spectra

Compounds **1** and **2a–c** slightly dissolve in water. In order to study the solution optical property of these four compounds, they were dissolved in water, heated at 60 °C for 20 min, then slowly cooled to room temperature. The UV spectra of **1**, **2a–c** were measured in the aqueous solution at room temperature in the region of 400–190 nm. The UV spectra exhibit one strong intensity absorption peak at 198 nm for **1**, 197 nm for **2a**, 197 nm for **2b**, 196 nm for **2c**, which are associated with the O_d–W charge transfer transitions, whereas the medium wide energy band appear at 256 nm for **1**, 271 and 279 nm for **2a**, 270 and 278 nm for **2b**, 271 and 277 nm for **2c**, which are due to $O_{b(c)}$–W charge transfer transitions, which are characteristic of Keggin-type polyoxoanion [15]. For **1**, one wide shoulder absorption band attributed to $O_{b(c)}$–W charge transitions is observed at 256 nm in the UV spectrum, the reason of which may be related to the covalent bonding interactions between the polyoxoanions and metal-organic cations (see Fig. S6).

3.3.3. Thermogravimetric analyses

To investigate the thermal stabilities for **1**, **2a–c**, TGA measurements were performed. Compound **1** shows three weight loss steps. The weight loss of 3.20% from 40 to 90 °C is attributed to the loss of six crystallographic water and two coordinated water (calculated value: 3.26%). The weight loss of 4.15% corresponds to the loss of the other coordinated water between 90 and 190 °C (calculated value: 4.08%). The weight loss of 3.68% from 260 to 340 °C is assigned to the loss of one pdc molecule (calculated value: 3.78%). Then, the decomposition of the framework compound **1** occurs starting at 340 °C. Compound **2a** shows the weight loss of 7.41% (calculated value: 7.34%) from 30 to 230 °C being ascribed to the release of all lattice water molecules and coordinated water. Then the quickly decomposition of the framework compound **2a** occurs starting at 590 °C. Compounds **2b** and **2c** exhibit the similar weight loss stages as compound **2a** (see Fig. S7).

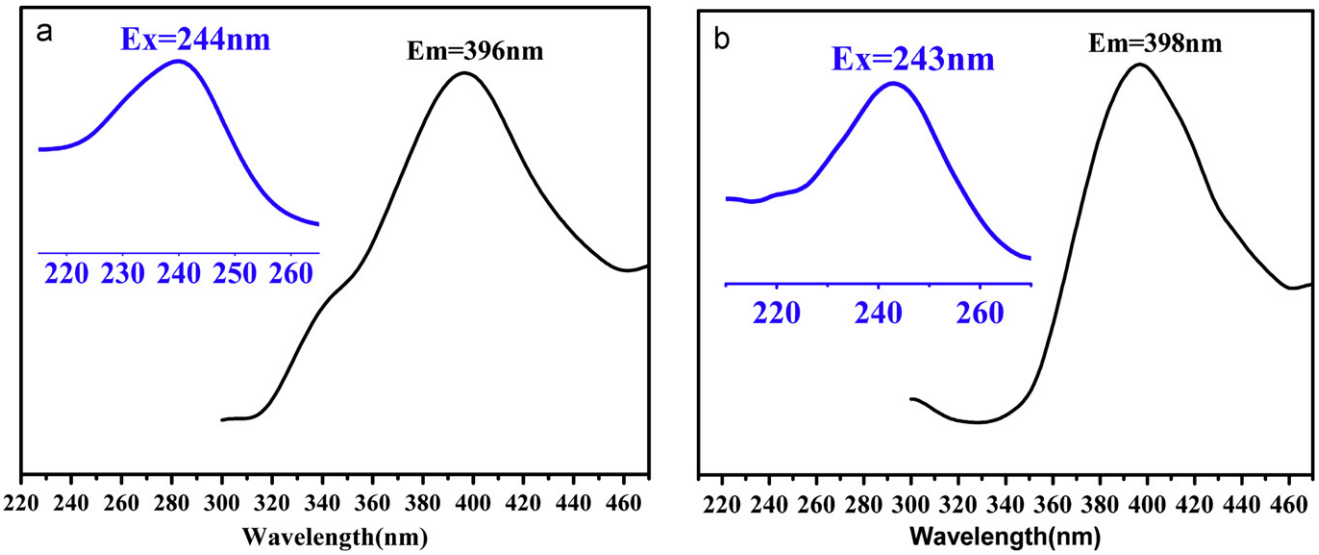

Fig. 7. (a) Emission spectrum (maximum 396 nm) and excitation spectrum (inset, maximum 244 nm) for **1**. (b) Emission spectrum (maximum 398 nm) and excitation spectrum (inset, maximum 243 nm) for **2a** in the solid state at room temperature.

3.3.4. *Powder X-ray diffraction*

The PXRD patterns indicate that the as-synthesized compounds match with the simulated one (see Fig. S8). Encouraged by the single crystal X-ray diffraction results, which reveal large free spaces within the framework of compounds **2a–c** (only **2a** is described in detail here), we carried out powder X-ray diffraction experiment to investigate the stability of compound **2a** upon the removal of guest molecules depending on TG analysis. The PXRD patterns indicate that the as-synthesized compound matches with the simulated one except for some intensity difference. After heating at 300 and 520 °C for 1 h, respectively, the color of the sample changes from orange to brown, and all the lattice water molecules and coordinated water are lost, according to TG analysis. The sample heated at 300 °C is treated in water for 12 h, and the color of the sample returns to orange again. The PXRD patterns of three samples remain essentially identical to those of the as-synthesized and simulated compound **2a**, as shown in Fig. 6. The sample heated at 520 °C seems to lose crystallinity and collapse; this cannot be reversed after the treatment in water for 24 h because of the broadening and decrease of intensity of the peaks, thus producing an amorphous phase upon heating.

3.3.5. *Photoluminescence properties*

The emission and excitation spectra of **1** and **2a** in solid state at room temperature are depicted in Fig. 7. These two compounds exhibit obvious photoluminescence with abroad emission band at 396 nm upon excitation at about 244 nm for **1** and 398 nm upon excitation at about 243 nm for **2a**, respectively. Compounds **2b** and **2c** have the similar photoluminescent behaviors as the compounds **1** and **2a**. The resemblance among the four compounds and H_2pdc implies that the luminescent behavior is ligand-based emission (compounds **2b** and **2c** are described as examples, see Fig. S9). Whereas, compared with that of H_2pdc [36], the maximum emission bands of compounds **2b** and **2c** are blue-shifted. The blue-shift of emission may be ascribed to the chelating of the H_2pdc ligand to the metal ion, which effectively enhances the rigidity of the ligand and reduces the loss of energy by radiationless decay of the intraligand emission exited state [22].

4. Conclusion

In summary, we have reported four novel inorganic–organic hybrid complexes. Compound **1** is a 3D pillar-layered framework with the $[SiW_{12}O_{40}]^{4-}$ anions located on the square voids of the two-dimensional bilayer sheets constructed from the H_2dipic ligands and Cerium(III) ions. Compounds **2a–c** are isostructural, which are constructed from 3D Ln-pdc-based MOF involving $[Ln(H_2O)_4(pdc)]_4^{4+}$ and noncoordinating guests Keggin structure $[SiW_{12}O_{40}]^{4-}$. They exhibited 3D non-interwoven frameworks with distorted-honeycomb cavities occupied by the Keggin $[SiW_{12}O_{40}]^{4-}$ polyoxoanion. The photoluminescent properties of compounds **1** and **2a–c** have been further investigated. Our research results indicate that, as a promising new type of multifunctional ligand, H_2pdc has a great potential in the field of coordination polymers, and further endeavors for exploration of H_2dpc complexes are underway in our workgroup. Future research may focus on attempting to explore the size effects of POM subunits. Further, it is reasonable to believe that the present work is important so as to expand on the application of these kinds of materials in molecular adsorption. These efforts are currently ongoing.

Acknowledgments

This work was financially supported by the Natural Science Fund Council of China (NSFC, nos. 20671011, 20701011, 20731002, 10876002, 20801004 and 20801005), Specialized Research Fund for the Doctoral Program of Higher Education (SRFDP, no. 200800070015), Open Fund of State Key Laboratory of Explosion Science and Technology, Beijing Institute of Technology (no. ZDKT08-01), China Postdoctoral Science Foundation (20070410037, 200801045).

Appendix A. Supplementary material

Supplementary data associated with this article can be found in the online version at doi:10.1016/j.jssc.2010.03.006.

References

[1] V. Soghomonian, Q. Chen, R.C. Haushalter, J. Zubieta, C.J. O'Connor, Science 259 (1993) 1596.
[2] K. Fukaya, T. Yamase, Angew. Chem. Int. Ed. 42 (2003) 654.
[3] D.L. Long, Y.F. Song, E.F. Wilson, P. Kgerler, S.X. Guo, A.M. Bond J.S.J. Hargreaves, L. Cronin, Angew. Chem. Int. Ed. 47 (2008) 4384.
[4] H.Q. Tan, Y.G. Li, Z.M. Zhang, C. Qin, X.L. Wang, E.B. Wang, Z.M. Su, J. Am. Chem. Soc. 129 (2007) 10066.
[5] L.H. Bi, E.V. Chubarova, N.H. Nsouli, M.H. Dickman, U. Kortz, B. Keita, L. Nadjo, Inorg. Chem. 45 (2006) 8575.
[6] C.-Y. Sun, S.-X. Liu, D.-D. Liang, K.-Z. Shao, Y.-H. Ren, Z.-M. Su, J. Am. Chem. Soc. 131 (2009) 1883.
[7] J.W. Cheng, S.T. Zheng, E. Ma, G.Y. Yang, Inorg. Chem. 46 (2007) 10534.
[8] J. Lu, Y. Xu, N.K. Goh, L.S. Chia, Chem. Commun. 21 (1998) 2733.
[9] M.I. Khan, E. Yohannes, R.J. Doedens, Angew. Chem. Int. Ed. 38 (1999) 1292.
[10] H.Y. An, E.B. Wang, D.R. Xiao, Y.G. Li, Z.M. Su, L. Xu, Angew. Chem. Int. Ed. 45 (2006) 904.
[11] S.-T. Zheng, J. Zhang, G.-Y. Yang, Angew. Chem. Int. Ed. 47 (2008) 3909.
[12] Z.G. Han, Y.Z. Gao, C.W. Hu, Cryst. Growth Des. 8 (2008) 1261.
[13] L.M. Zheng, Y.S. Wang, X.Q. Wang, J.D. Korp, A.J. Jacobson, Inorg. Chem. 40 (2001) 1380.
[14] A.-X. Tian, J. Ying, J. Peng, J.-Q. Sha, Z.-G. Han, J.-F. Ma, Z.-M. Su, N.-H. Hu H.-Q. Jia, Inorg. Chem. 47 (2008) 3274.
[15] J.W. Zhao, Y.P. Song, P.T. Ma, J.P. Wang, J.Y. Niu, J. Solid State Chem. 182 (2009) 1798.
[16] X.L. Wang, Y.F. Bi, B.K. Chen, H.Y. Lin, G.C. Liu, Inorg. Chem. 47 (2008) 2442.
[17] Z.G. Han, Y.L. Zhao, J. Peng, A.X. Tian, Y.H. Feng, Q. Liu, J. Solid State Chem. 178 (2005) 1386.
[18] X.J. Kong, Y.P. Ren, P.Q. Zheng, Y.X. Long, L.S. Long, R.B. Huang, L.S. Zheng, Inorg. Chem. 45 (2006) 10702.
[19] S.L. Li, Y.Q. Lan, J.F. Ma, J. Yang, X.H. Wang, Z.M. Su, Inorg. Chem. 46 (2007) 8283.
[20] J. Lü, E.H. Shen, Y. Li, D.R. Xiao, E.B. Wang, L. Xu, Cryst. Growth Des. 5 (2005) 65.
[21] M.L. Wei, C. He, Q.Z. Sun, Q.J. Meng, C.Y. Duan, Inorg. Chem. 46 (2007) 5957.
[22] C.-H. Li, K.-L. Huang, Y.-N. Chi, X. Liu, Z.-G. Han, L. Shen, C.-W. Hu, Inorg. Chem. 48 (2009) 2010.
[23] L.-Z. Zhang, W. Gu, Z.-L. Dong, X. Liu, B. Li, M.-L. Liu, J. Solid State Chem. 182 (2009) 1040.
[24] M. Sheldrick, SHELXS-97, Programs for Crystal Structure Solution, University of Göttingen, Göttingen, Germany, 1997.
[25] G.M. Sheldrick, SHEXTL-97, Programs for Crystal Structure Refinements, University of Göttingen, Germany, 1997.
[26] J.Q. Sha, J. Peng, A.X. Tian, H.S. Liu, J. Chen, P.P. Zhang, Z.M. Su, Cryst. Growth Des. 7 (2007) 2535.
[27] Z.G. Han, T. Chai, Y.N. Wang, Y.Z. Gao, C.W. Hu, Polyhedron 29 (2010) 196.
[28] T. Howard, J. Evans, M.T. Pope, Inorg. Chem. 23 (1984) 501.
[29] M.T. Pope, Heteropoly and Isopoly Oxometalates, Springer, Berlin, 1983.
[30] C. Streb, D.-L. Long, L. Cronin, Chem. Commun. (2007) 471.
[31] D. Hagrman, P.J. Hagrman, J. Zubieta, Angew. Chem. Int. Ed. 38 (1999) 3165.
[32] J.J. Pluth, J.V. Smith, J.M. Bennett, J. Am. Chem. Soc. 111 (1989) 1692.
[33] Y.Q. Tian, Y.M. Zhao, Z.X. Chen, G.N. Zhang, L.H. Weng, D.Y. Zhao, Chem. Eur. J. 13 (2007) 4146.
[34] I.D. Brown, D. Altermatt, Acta Crystallogr. Sect. B Sci. 41 (1985) 244.
[35] P.-Q. Zheng, Y.-P. Ren, L.-S. Long, R.-B. Huang, L.-S. Zheng, Inorg. Chem. 44 (2005) 1190.
[36] E.B. Wang, G.P. Wang, R.D. Huang, Sci. Bull. 37 (1992) 1195 (in Chinese).